

1 **Molecular Evolution of the Meiotic Recombination Pathway in Mammals**

2 *Investigations*

3

4 Amy L. Dapper^{1,2*} and Bret A. Payseur¹

5

6 ¹ Laboratory of Genetics, University of Wisconsin, Madison, WI 53706, USA

7 ² Department of Biological Sciences, Mississippi State University, Mississippi State, MS 39762, USA

8 Running Title: Evolution of the Recombination Pathway

9 Keywords: (up to 5)

10

11 * Corresponding Author : Amy L. Dapper

12 Address: 295 E. Lee Blvd., P.O. Box GY, Mississippi State, MS 39762

13 Phone: (662) 325-7575

14 Email: dapper@biology.msstate.edu

Abstract

Meiotic recombination, the exchange of genetic material between homologous chromosomes during meiosis, is required for successful gametogenesis in most sexually reproducing species. Recombination is also a fundamental evolutionary force, influencing the fate of new mutations and determining the genomic scale over which selection shapes genetic variation. Despite the central importance of recombination, basic questions about its evolution have yet to be addressed. Although many genes that play roles in recombination have been identified, the molecular evolution of most of these genes remains uncharacterized. Using a phylogenetic comparative approach, we measure rates of evolution in 32 recombination pathway genes across 16 mammalian species, spanning primates, murids, and laurasithians. By analyzing a carefully-selected panel of genes involved in key components of recombination – spanning double strand break formation, strand invasion, the crossover/non-crossover decision, and resolution – we generate a comprehensive picture of the evolution of the recombination pathway in mammals. Recombination genes exhibit marked heterogeneity in the rate of protein evolution, both across and within genes. We report signatures of rapid evolution and positive selection that could underlie species differences in recombination rate. **[NEEDS WORK HERE]**

Abstract Word Count : (< 250)

Introduction

The reciprocal exchange of DNA between homologous chromosomes during meiosis – recombination – is required for successful gametogenesis in most species that reproduce sexually (Hassold and Hunt 2001). The rate of recombination is a major determinant of patterns of genetic diversity in populations, influencing the fate of new mutations (Hill and Robertson 1966), the efficacy of selection (Felsenstein 1974; Charlesworth *et al.* 1993; Comeron *et al.* 1999; Gonen *et al.* 2017), and important features of the genomic landscape (Begun and Aquadro 1992; Charlesworth *et al.* 1994; Duret and Arndt 2008).

Although recombination rate is often treated as a constant, this fundamental parameter evolves over time. Genomic regions ranging in size from short sequences to entire chromosomes vary in recombination rate – both within and between species (Burt and Bell 1987; Broman *et al.* 1998; Jeffreys *et al.* 2005; Coop and Przeworski 2007; Kong *et al.* 2010; Dumont *et al.* 2011; Smukowski and Noor 2011; Comeron *et al.* 2012; Segura *et al.* 2013; Dapper and Payseur 2017; Stapley *et al.* 2017).

Genome-wide association studies are beginning to reveal the genetic basis of differences in recombination rate within species. Individual recombination rates have been associated with variation in specific genes in populations of *Drosophila melanogaster* (Hunter *et al.* 2016), humans (Kong *et al.* 2008, 2014; Chowdhury *et al.* 2009; Fledel-Alon *et al.* 2011), domesticated cattle (Sandor *et al.* 2012; Ma *et al.* 2015; Kadri *et al.* 2016; Shen *et al.* 2018), domesticated sheep (Petit *et al.* 2017), Soay sheep (Johnston *et al.* 2016), and red deer (Johnston *et al.* 2018). Variants in several of these genes correlate with recombination rate in multiple species, including: *Rnf212* (Kong *et al.* 2008; Chowdhury *et al.* 2009; Fledel-Alon *et al.* 2011; Sandor *et al.* 2012; Johnston *et al.* 2016; Kadri *et al.* 2016; Petit *et al.* 2017), *Rnf212B* (Johnston *et al.* 2016, 2018; Kadri *et al.* 2016), *Rec8* (Sandor *et al.* 2012; Johnston *et al.* 2016, 2018), *Hei10/Ccnb1ip1* (Kong *et al.* 2014; Petit *et al.* 2017), *Msh4* (Kong *et al.* 2014; Ma *et al.* 2015; Kadri *et al.* 2016; Shen *et al.* 2018), *Cplx1* (Kong *et al.* 2014; Ma *et al.* 2015; Johnston *et al.* 2016; Shen *et al.* 2018) and *Prdm9* (Fledel-Alon *et al.* 2011; Sandor *et al.* 2012; Kong *et al.* 2014; Ma *et al.* 2015; Shen *et al.* 2018).

In contrast, the genetics of recombination rate variation among species remains poorly understood. Divergence at the di-cistronic gene *mei-217/mei-218* explains much of the disparity in genetic map length between *D. melanogaster* and *D. mauritiana* (Brand *et al.* 2018). *mei-217/mei-218* is the only gene known to confer a recombination rate difference between species, though quantitative trait loci that contribute to shifts in rate among subspecies of house mice have been identified (Dumont and Payseur 2010; Murdoch *et al.* 2010; Balcova *et al.* 2016).

One strategy for understanding how species diverge in recombination rate is to inspect patterns of molecular

evolution at genes involved in the recombination pathway. This approach incorporates knowledge of the molecular and cellular determinants of recombination and is motivated by successful examples. *mei-217/mei-218* was targeted for functional analysis based on its profile of rapid evolution between *D. melanogaster* and *D. mauritiana* (Brand *et al.* 2018). *Prdm9*, a protein that positions recombination hotspots in house mice and humans through histone methylation (Myers *et al.* 2010; Parvanov *et al.* 2010; Grey *et al.* 2011, Paigen2018; 2018), shows accelerated divergence across mammals (Oliver *et al.* 2009). The rapid evolution of *Prdm9* – which localizes to its zinc-finger DNA binding domain (Oliver *et al.* 2009) – appears to be driven by selective pressure to recognize new hotspot motifs as old ones are destroyed via biased gene conversion (Myers *et al.* 2010; Ubeda and Wilkins 2011; Lesecque *et al.* 2014; Latrille *et al.* 2017). Although these examples demonstrate the promise of signatures of molecular evolution for illuminating recombination rate differences between species, patterns of divergence have yet to be reported for most genes involved in meiotic recombination.

Mammals provide a useful system for dissecting the molecular evolution of the recombination pathway for several reasons. First, the evolution of recombination rate has been measured along the mammalian phylogeny (Dumont and Payseur 2008; Segura *et al.* 2013). Second, recombination rate variation has been associated with specific genes in mammalian populations (Kong *et al.* 2008, 2014; Chowdhury *et al.* 2009; Sandor *et al.* 2012; Ma *et al.* 2015; Johnston *et al.* 2016, 2018; Kadri *et al.* 2016; Petit *et al.* 2017; Shen *et al.* 2018). Third, laboratory mice have proven to be instrumental in the identification and functional characterization of recombination genes (Vries *et al.* 1999; Baudat *et al.* 2000; Romanienko and Camerini-Otero 2000; Yang *et al.* 2006; Ward *et al.* 2007; Schramm *et al.* 2011; Bisig *et al.* 2012; Bolcun-Filas and Schimenti 2012; La Salle *et al.* 2012; Kumar *et al.* 2015; Finsterbusch *et al.* 2016; Stanzione *et al.* 2016) .

Work in mice indicates that the mammalian recombination pathway is roughly divided into five major steps, each of which is regulated by a handful of genes. The first step is the formation of hundreds of double strand breaks (DSBs) throughout the genome (Bergerat *et al.* 1997; Keeney *et al.* 1997; Baudat *et al.* 2000; Romanienko and Camerini-Otero 2000; Baudat and Massy 2007; Finsterbusch *et al.* 2016; Lange *et al.* 2016). After formation, DSBs are identified, processed, and paired with their corresponding location on the homologous chromosome through the processes of homology search and strand invasion (Keeney 2007; Cloud *et al.* 2012; Brown and Bishop 2014; Finsterbusch *et al.* 2016; Kobayashi *et al.* 2016; Oh *et al.* 2016; Xu *et al.* 2017). The pairing of homologous chromosomes is then stabilized by a proteinaceous structure referred to as the synaptonemal complex (SC) (Meuwissen *et al.* 1992; Schmekel and Daneholt 1995; Costa *et al.* 2005; Vries *et al.* 2005; Hamer *et al.* 2006; Yang *et al.* 2006; Schramm *et al.* 2011; Fraune *et al.* 2014; Hernández-Hernández *et al.* 2016). The SC also forms a substrate on which the eventual crossover

events will take place [citations]. It is at this point that a small subset of DSBs is designated to mature into crossovers, leaving the majority of DSBs to be resolved as non-crossovers (Snowden *et al.* 2004; Yang *et al.* 2008; Reynolds *et al.* 2013; Finsterbusch *et al.* 2016; Rao *et al.* 2017). Finally, this designation is followed, and each DSB is repaired as a crossover or a non-crossover (Baker *et al.* 1996; Edelman *et al.* 1996; Lipkin *et al.* 2002; Rogacheva *et al.* 2014; Xu *et al.* 2017).

In this article, we examine the molecular evolution of 32 key recombination genes, evenly distributed across each major step in the recombination pathway, in 16 mammalian species spanning Primates, Rodents and Laurasiatherians. In addition to revealing patterns of divergence across diverse mammalian species, we leverage human polymorphism data to make robust evolutionary inferences. Our results provide a comprehensive picture of evolution in the recombination pathway in mammals and identify steps of the pathway most likely to contribute to differences in recombination rate between species.

Materials and Methods

Data Acquisition & Processing

We selected a focal panel of 32 recombination genes (See Table1). The panel was constructed to: (1) cover each major step in the recombination pathway as evenly as possible, (2) contain genes that have integral functions in each step, and (3) include genes that have been associated with inter-individual differences in recombination rate within mammalian populations. Reference sequences were downloaded for each gene in 16 mammalian species from both NCBI and Ensembl (Release-89)(Wheeler *et al.* 2006; Zerbino *et al.* 2017).

Alternative splicing is widespread and presents a challenge for molecular evolution studies (Pan *et al.* 2008; Barbosa-Morais *et al.* 2012). To focus our analyses on coding sequences that are transcribed during meiosis and to validate the computational annotations for each gene in each species, we used available testes expression datasets. We downloaded raw testes expression data for each mammalian species from NCBI Gene Expression Omnibus (GEO) (Table S1)(Barrett *et al.* 2012). We converted the SRA files into FASTQ files using SRAToolkit (Leinonen *et al.* 2010). The reads were mapped to an indexed reference genome (Table S2,3) (Bowtie2, (Langmead and Salzberg 2012)) using TopHat (Trapnell *et al.* 2009). The resulting bam files were sorted using Samtools (Li *et al.* 2009) and visualized using IGV 2.4.10 (Thorvaldsdóttir *et al.* 2013). This allowed us to: (1) identify the transcript expressed in testes, (2) check the reference transcript for errors, and (3) revise the reference transcript based upon the transcript data.

We compared expression data to annotations from both Ensembl and NCBI (Wheeler *et al.* 2006; Zerbino *et*

al. 2017). When both transcripts were identical, we selected the NCBI transcript. The Ensembl transcript was used instead when: (1) the NCBI reference sequences was not available for a given gene in a given species, (2) when none of the NCBI transcripts matched the expression data, or (3) when there were sequence differences between the two transcripts and the Ensembl transcript was more parsimonious - i.e. had the fewest differences when compared to the rest of sequences in the alignment. The use of testes expression data was a key data processing step and the inclusion of species in this study was primarily determined by the availability of testes expression data.

Phylogenetic Comparative Approach in Mammals

For each gene, we used phylogenetic analysis by maximum likelihood (PAML 4.8) to measure the rate of evolution across the mammalian phylogeny and to search for molecular signatures indicative of positive selection (Table 2) (Yang 1997, 2007). This approach requires a sequence alignment and a phylogenetic tree. For each gene, sequences were aligned using Translator X, a codon-based alignment tool, powered by MUSCLE v3.8.31 (Edgar 2004; Abascal *et al.* 2010). Each alignment was examined by hand and edited as necessary. We used a species tree that reflects current understanding of the phylogenetic relationships of the species included in our study (Figure 1)(Prasad *et al.* 2008; Perelman *et al.* 2011; Fan *et al.* 2013; Chen *et al.* 2017).

Due to the ambiguity in the relationship between Laurasithians and the placement of tree shrews, we also inferred gene trees using MrBayes (Ronquist *et al.* 2012; Fan *et al.* 2013; Chen *et al.* 2017). This approach also allowed us to control for effects of incomplete lineage sorting (ILS) (Pamilo and Nei 1988; Rosenberg 2002; Scornavacca and Galtier 2017). Using gene trees and using the consensus species tree produced highly similar results (Table S4).

For the majority of genes, transcripts from all 16 species were used (19 genes). However, for a number of genes, the chimpanzee and bonobo sequences were identical, in which case only the chimpanzee sequence was included in the analyses (11 genes). In one case, the chimpanzee, bonobo and human sequences were all identical, in which case only the human sequence was included in the analyses. In only a small number of instances, a suitable reference sequence could not be identified for a given species.

We estimated rates of synonymous and non-synonymous substitutions per site using the CODEML program in PAML4.8 (Yang 2007). This program considers multiple substitutions per site, different rates of transitions and transversions, and effects of codon usage (Yang 2007). Rates of substitution were computed for 6 different models of molecular evolution (Table 2). The fit of each model was compared using a likelihood ratio test.

Reported substitution rates assume the best-fit model for each gene.

Identifying Signatures of Selection

To test for positive selection, we compared the fit of models including a class of sites with ω greater than 1 to the fit of models in which all classes of sites have ω values equal to, or less than, 1. Specifically, we report three comparisons: M1 vs. M2, M7 vs. M8, M8 vs. M8a (Table 2). The first comparison, M1 vs. M2, compares a model with two classes of sites ($\omega < 1$, $\omega = 1$) to a model with a third class of sites where ω is greater than 1, indicative of positive selection (Yang 2007). More complex models (M7 & M8) were developed to take into account variation in ω less than one among sites within genes and thus, include 10 site classes drawn from a beta distribution between 0 and 1 (Yang 2007). In this case, Model 8 includes an additional 11 class of sites in which ω is greater than 1, allowing for the identification of signatures of positive selection (Yang 2007). In cases in which a large fraction of sites within a gene are evolving neutrally ($\omega = 1$), Model 8 will fit significantly better due to a very poor fit of Model 7 rather than a signature of positive selection. To avoid incorrectly identifying signature of positive selection, Model 8 is also compared to Model 8a which contains a larger fraction of neutrally evolving sites than Model 7 [citations].

Multinucleotide Mutations

Multi-nucleotide mutations (MNM) occur when two mutations happen simultaneously in close proximity (Schridder *et al.* 2011; Besenbacher *et al.* 2016). MNMs violate the PAML assumption that the probability of two simultaneous mutations in the same codon is 0 (Yang 2007; Venkat *et al.* 2018). Recent work has shown that MNMs can falsely detect positive selection when using branch-site tests in PAML (Venkat *et al.* 2018). Although we did not use branch-site tests, it is possible that MNMs contributed to some of the signatures of positive selection we observed. We could not directly identify MNMs in our dataset. Instead, we identified codons with multiple differences (CMDs) that likely arose on a single branch of the phylogeny. We used PAML to reconstruct the ancestral sequence at each node in the phylogeny (Yang 2007). For the reconstruction, Model 8 was chosen because we specifically re-analyzed genes that showed evidence for positive selection when comparing Model 7 with Model 8. From the ancestrally reconstructed sequences, we identified any codons in which PAML inferred more than 1 substitution on a single branch. All identified CMDs were removed from the sequences in which they occurred. For example, if a CMD was identified in an external branch, that codon was replaced with ‘—’ only in the sequence of that species. If a CMD was inferred on an internal branch, the codon was replaced with ‘—’ in all species descended from that internal branch. For

each gene that showed evidence of positive selection using the unedited sequences, we also conducted PAML analyses using sequences from which all CMDs were removed.

Polymorphism & Divergence in the Primate Lineage

To further examine evidence for selection on recombination genes, we compared divergence between humans and macaque to polymorphism within humans in 29 recombination genes. Human polymorphism data was downloaded from ExAC database. Polymorphism data was not available for 3 genes (*RNF212*, *MEI4*, and *REC8*), and thus these genes were not included in this analysis. By comparing counts of non-synonymous and synonymous polymorphisms to counts of non-synonymous and synonymous substitutions using the McDonald-Kreitman test, we can identify either an excess of non-synonymous substitutions, indicative of positive selection, or a paucity of non-synonymous substitutions, indicative of negative selection [citation]. Additionally, pairwise divergence between humans and macaques was calculated using yn00 package in PAML (Yang 2007).

Identifying Evolutionary Patterns

To identify evolutionary patterns among our recombination genes, we compared the rate of evolution and the proportion of genes experiencing positive selection among groups of interest. We asked: (1) Do genes that function in different steps of the pathway exhibit different rates of evolution? (2) Do genes that function post-synapsis evolve more rapidly than genes that function pre-synapsis? and (3) Do genes associated with between-individual variation in recombination rate diverge more rapidly between species? All statistical analyses were performed in R [citation].

Evolutionary rate covariation (ERC) metric is the correlation coefficient between branch-specific rates between two proteins (Clark *et al.* 2012). ERC is typically elevated among interacting proteins and is assumed to result from: (1) concordance in fluctuating evolutionary pressures, (2) parallel evolution of expression level, or (3) compensatory changes between co-evolving genes (Clark *et al.* 2012, 2013). We used a publicly available ERC dataset (https://csb.pitt.edu/erc_analysis/index.php) to compare the median ERC-value among a subset of our focal recombination genes ($N = 25$) to the genome as a whole, as described in (Priedigkeit *et al.* 2015).

To control for this general elevation in ERC among recombination genes and test for relationships between specific groups between them, we calculated ERC values for only our focal set of 32 recombination genes. Branch lengths were calculated using aaML package in PAML (Yang 2007) and pairwise ERC values were

calculated following the methods of (Clark *et al.* 2012). Using this approach, we specifically compared the ERC values among three of the most rapidly evolving recombination genes (*TEX11*, *SHOC1*, and *SYCP2*).

Results

Heterogeneity in evolutionary rate among recombination genes

We observed substantial heterogeneity in the rate of evolution of recombination genes, spanning a range of 0.0268 – 0.8483 (mean $\omega = 0.3275$, SD = 0.1971, median = 0.30945) (Figure 2A, Figure 3, Table 3). Four genes exhibit particularly rapid evolution compared to other recombination genes, having evolutionary rates greater than 1 SD above mean (*SYCP2*, *TEX11*, *SHOC1*, *IHO1*). At the other end of the spectrum, five genes have evolutionary rates more than 1 SD below mean and are highly conserved across the mammalian phylogeny (*BRCC3*, *HEI10*, *DMC1*, *RAD51*, *RAD50*). In general, there is very high concordance between evolutionary rate across mammals and pairwise divergence between humans and macaques (mean $\omega = 0.3301$, SD = 0.2370, median = 0.30925) (Figure 2B, Table 4). It should be noted, however, that these two measures are not independent - divergence between human and macaque sequences is incorporated in the phylogenetic analysis. Six genes have evolutionary rates more than 1 SD above mean (*CNTD1*, *TEX11*, *SHOC1*, *IHO1*, *MEI4*, *RAD21L*). Likewise, six genes have evolutionary rates more than 1 SD below mean (*HORMAD1*, *MRE11*, *RAD50*, *DMC1*, *RAD51*, *MLH1*).

The genes that show the most rapid and most conserved rates of divergence between humans and macaques largely, but not completely, overlaps with the genes showing extreme evolutionary rates across the mammalian phylogeny. There are a few notable outliers that show much more rapid divergence between humans and macaques than across the mammalian phylogeny as a whole. These include *MEI4* ($\omega_{\text{mammals}} = 0.4332$, $\omega_{\text{human-macaque}} = 0.7252$), *CNTD1* ($\omega_{\text{mammals}} = 0.2496$, $\omega_{\text{human-macaque}} = 0.6803$), and *HEI10* ($\omega_{\text{mammals}} = 0.1226$, $\omega_{\text{human-macaque}} = 0.3235$).

Elevated evolutionary rate among recombination genes

Gradnigo et al. (2016) measured the rate of divergence between human and macaque for 3,606 genes throughout the genome. We used this dataset to ask whether the rate of evolution of recombination genes as a group is different than expected from the genome-wide distribution. We randomly sampling 32 ω values from this larger dataset and asked how frequently we observed average evolutionary rates as high or higher than observed among our focal set of recombination genes (mean $\omega = 0.3301$). We found evidence for a

significantly elevated evolutionary rate among recombination genes, observing a mean as high (or higher) than the value observed among recombination genes less than 1% of the time ($p = 0.0075$, sample size = 10,000) (Figure 4).

Evidence of positive selection across the mammalian phylogeny

We identified signatures of positive selection in 10 recombination genes (31.25%) using site models in CODEML. These genes include: *IHO1*, *MRE11*, *SYCP1*, *SYCP2*, *REC8*, *RAD21L*, *RNF212*, *TEX11*, *MSH4*, *SHOC1* (Table 2). For each of these genes, models that include a fraction of sites where the rate of non-synonymous substitutions is estimated to be greater than the rate of synonymous substitutions ($\omega > 1$, Model 8) had a significantly better fit than models that did not include such a class of sites (Model 7, 8a). Due to the potential for multi-nucleotide mutations to produce erroneous signatures of positive selection, we re-analyzed this subset of genes removing any codons inferred to have accumulated multiple changes on a single branch (CMDs). After removing all CMDs, 1 gene (*TEX11*) retained a significant signature of positive selection (Table 5).

Comparing polymorphism within humans to divergence between humans and macaques revealed a general pattern of negative selection among recombination genes in the primate lineage. A majority of the recombination genes (16 genes, 55.17%) had a significant paucity of non-synonymous substitutions, indicative of negative (purifying) selection (Fisher’s Exact Test, Table 4). None of the genes had a significant excess of non-synonymous substitutions, which would indicate a significant signature of positive selection. Only one gene (*TEX11*) had a positive alpha score ($\alpha = 0.2929$) and a corresponding neutrality index less than 1 ($NI = 0.7071$), indicating a higher fraction of non-synonymous substitutions than non-synonymous polymorphisms (Table 4).

Recombination genes associated with inter-individual differences do not diverge more rapidly between species

We did not find evidence that recombination genes associated with inter-individual differences in recombination rate evolve more rapidly than other recombination genes. While we observed a higher mean evolutionary rate among genes associated with inter-individual differences ($\omega = 0.3943$ v. $\omega = 0.2925$, respectively), the difference was not significant ($p = 0.2381$, Mann-Whitney U Test). Likewise, we observed a greater proportion of genes associated with inter-individual variation exhibited signatures of positive selection (5/11 vs. 5/21, respectively), this difference was also not significant ($p = 0.210$, Chi-Squared Test). The difference

in evolution rates between these two classes of genes was greater when considering only divergence between humans and macaques ($\omega = 0.4181$ vs. $\omega = 0.2839$) ($p = 0.08816$, Mann-Whitney U Test).

Genes that function post-synapsis are more likely to exhibit signatures of positive selection

We did not find evidence that recombination genes that in different steps of the pathway exhibit different evolutionary rates. This was the case both when comparing the 6 major steps in the recombination pathway ($p = 0.1422$, Kruskal-Wallis Test)(Figure 6) and when comparing more generally between genes that function pre- and post-synapsis ($\omega = 0.3762$ vs. $\omega = 0.2723$, respectively) ($p = 0.1425$, Mann-Whitney U Test). Likewise, we didn't observed significant differences between recombination genes by step in the pathway when comparing just divergence between humans and macaques ($p = 0.1422$, Kruskal-Wallis Test). However, the rate of divergence between humans and macaques of post-synapsis genes was borderline significantly higher when compared to pre-synapsis recombination genes ($\omega = 0.3994$ v. $\omega = 0.2514$, respectively) ($p = 0.05827$, Mann-Whitney U Test). Interestingly, we did observe that a significantly higher fraction of post-synapsis recombination genes exhibited signatures of positive selection in comparison with pre-synapsis recombination genes (8/17 v. 2/15, respectively) ($p = 0.03998$, Chi-Squared Test).

Evolutionary rates among recombination genes are correlated

Meiotic genes have been shown to exhibit statistically significant, but not strong, ERC among mammals (Clark *et al.* 2013). Similarly, we identified significant evidence for correlated evolution among genes in the recombination pathway (mean ERC = 0.134, permutation $p = 0.000358$). After factoring out the general elevation of ERC values among recombination genes, the mean ERC value among our focal set of genes was approximately zero (mean ERC = 0.000358). Among recombination genes, we detected strong signature of correlated evolution between our three genes of interest: *SHOC1*, *TEX11*, *SYCP2* (mean ERC = 0.42369, permutation $p = 0.025$). Thus, the coevolutionary pattern among these three genes is statistically stronger than that observed generally among recombination genes.

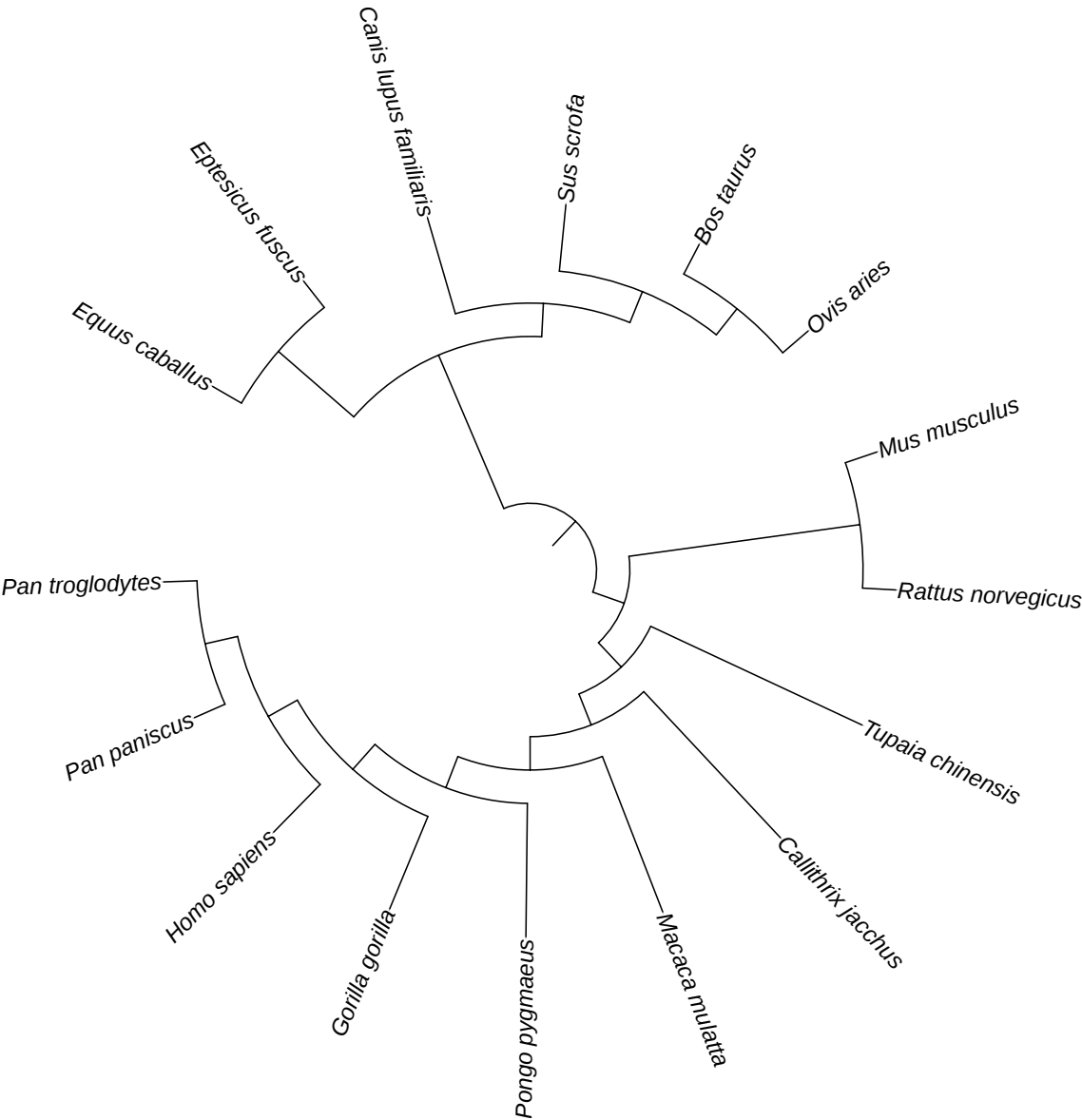
291 **Table 1** : List of 32 recombination genes surveyed by step in the recombination pathway. Genes in bold have
292 been associated with inter-individual differences in recombination rate in at least one species of mammals.

Pathway Step	Genes
DSB Formation	<i>HORMAD1</i> , <i>MEI4</i> , <i>REC114</i> , <i>IHO1</i> , <i>SPO11</i>
DSB Processing	<i>HORMAD2</i> , <i>MRE11</i> , <i>NBS1</i> , <i>RAD50</i> , <i>BRCC3</i>
Strand Invasion	<i>DMC1</i> , <i>RAD51</i> , <i>SPATA22</i> , <i>MEIOB</i> , <i>MCMDC2</i>
Homologous Pairing	<i>REC8</i> , <i>RAD21L</i> , <i>SYCP1</i> , <i>SYCP2</i> , <i>TEX11</i>
CO vs. NCO Decision	<i>TEX11</i> , <i>SHOC1</i> , <i>RNF212</i> , <i>RNF212B</i> , <i>MSH4</i> , <i>MSH5</i>
Resolution	<i>MER3</i> , <i>CNTD1</i> , <i>HEI10</i> , <i>MLH1</i> , <i>MLH3</i> , <i>MUS81</i>

293 **Table 2**: Six PAML site models used to measure evolutionary rate and test for positive selection. Models
294 varied in the number of ω classes, the range of ω for each of these classes, and whether a class of sites subject
295 to positive selection was included.

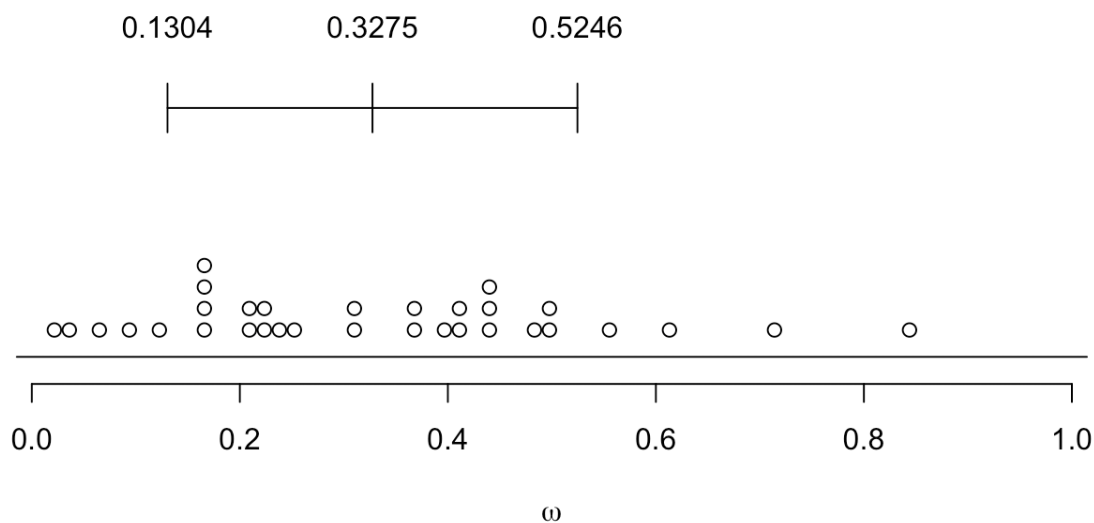
Model	# Site Classes	ω Range	Pos. Selection?
0	1	<1	No
1	2	<1, =1	No
2	3	<1, =1, >1	Yes
7	10	0-1	No
8	11	0-1, >1	Yes
8a	6	0-1, =1	No

Figure 1: Species tree assumed in analyses of molecular evolution.



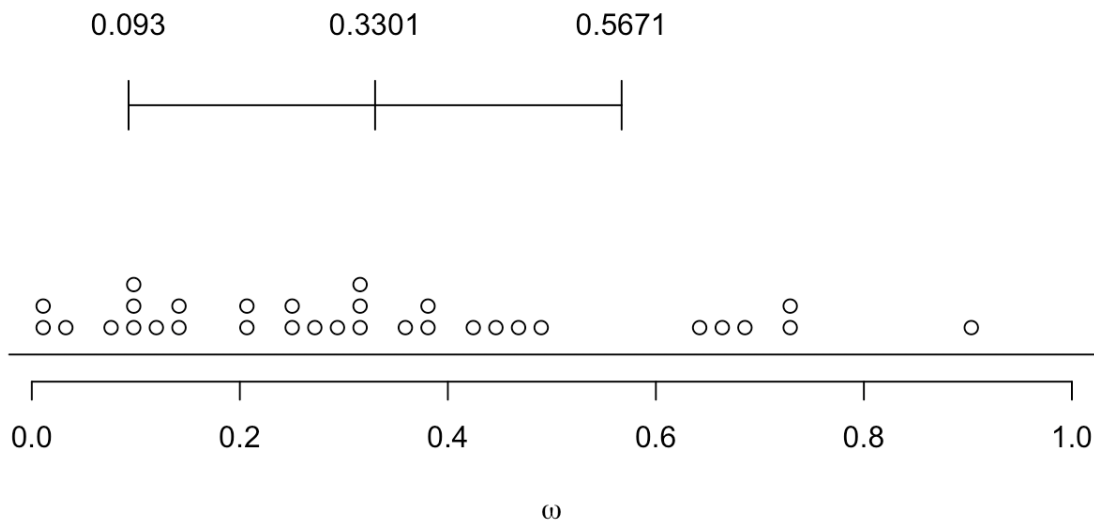
298 **Figure 2:** Distribution of ω for 32 recombination genes. Bar shows the mean \pm 1 standard deviation.
 299 (A) Divergence estimated across the mammalian phylogeny. (B) Pairwise divergence between human and
 300 macaque.

301 (A)



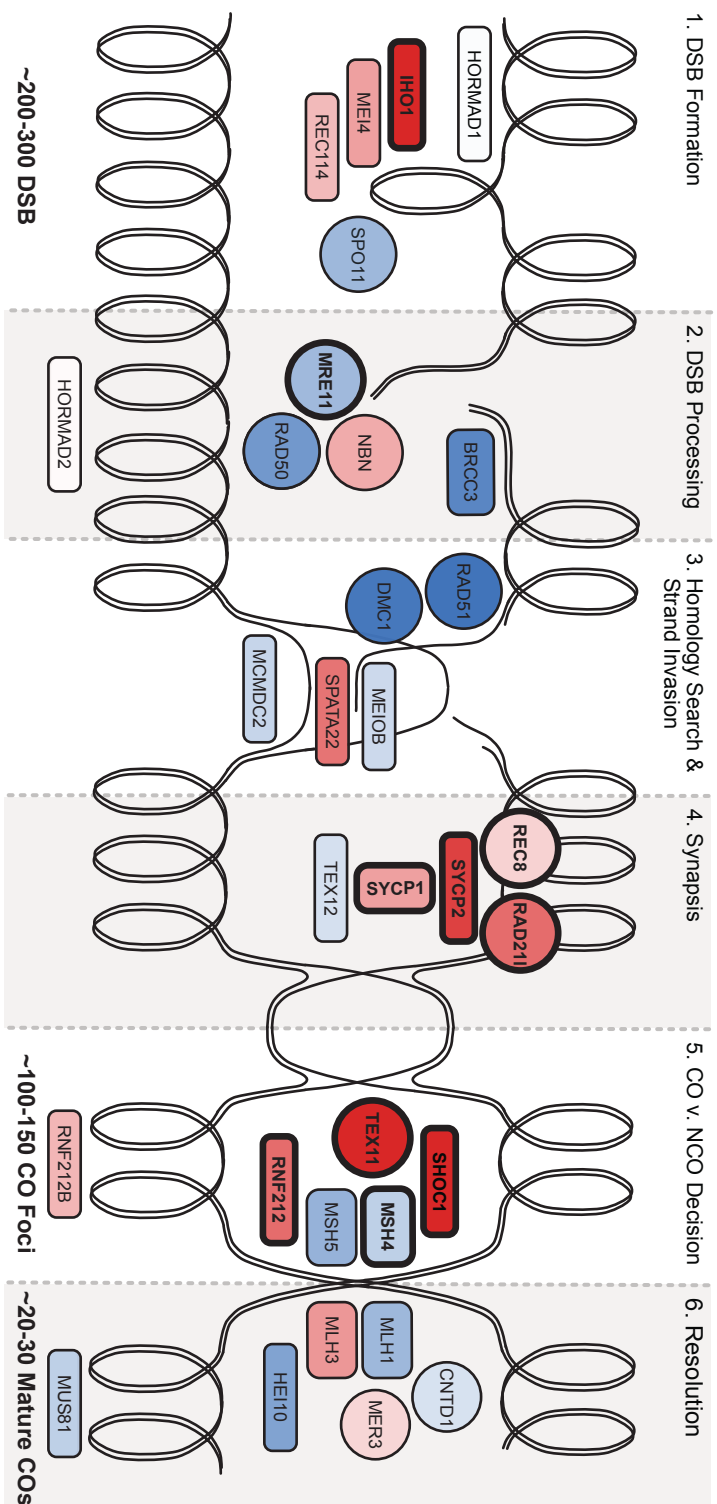
302

303 (B)

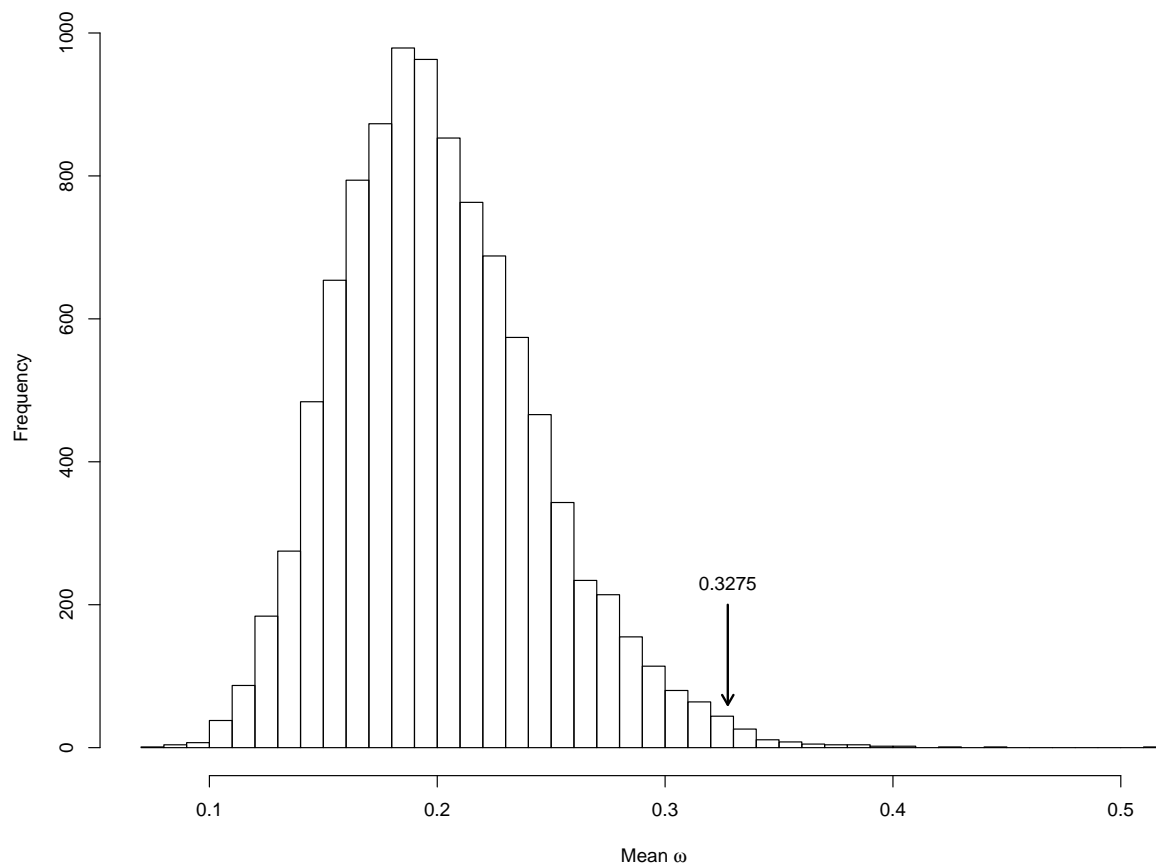


304

Figure 3: Pathway Figure Description The color of each gene represents its evolutionary rate relative to the average rate of evolution of recombination genes ($\omega = 0.3275$): more rapidly evolving genes are depicted in darker shades of red and the more conserved genes are depicted in darker shades of blue. Genes that exhibit a signature of positive selection are in bold.

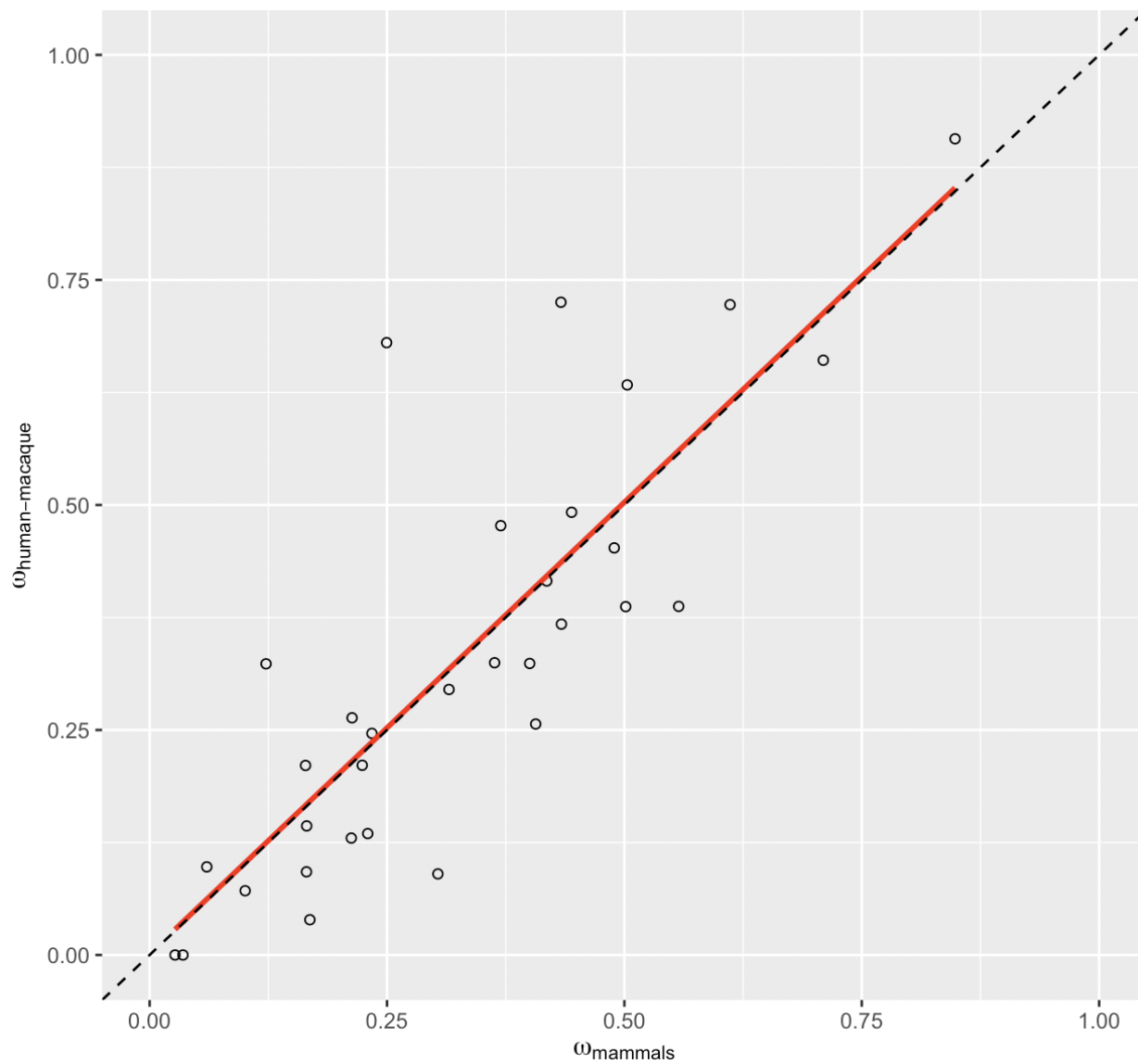


310 **Figure 4:** Distribution of the mean divergence (ω) between human and macaque of 10,000 random draws
 311 from the entire genome. Mean ω among these random draws was observed to be equal to or greater than
 312 that observed among recombination genes less than 1% of the time ($p = 0.0075$, 10,000 random draws).



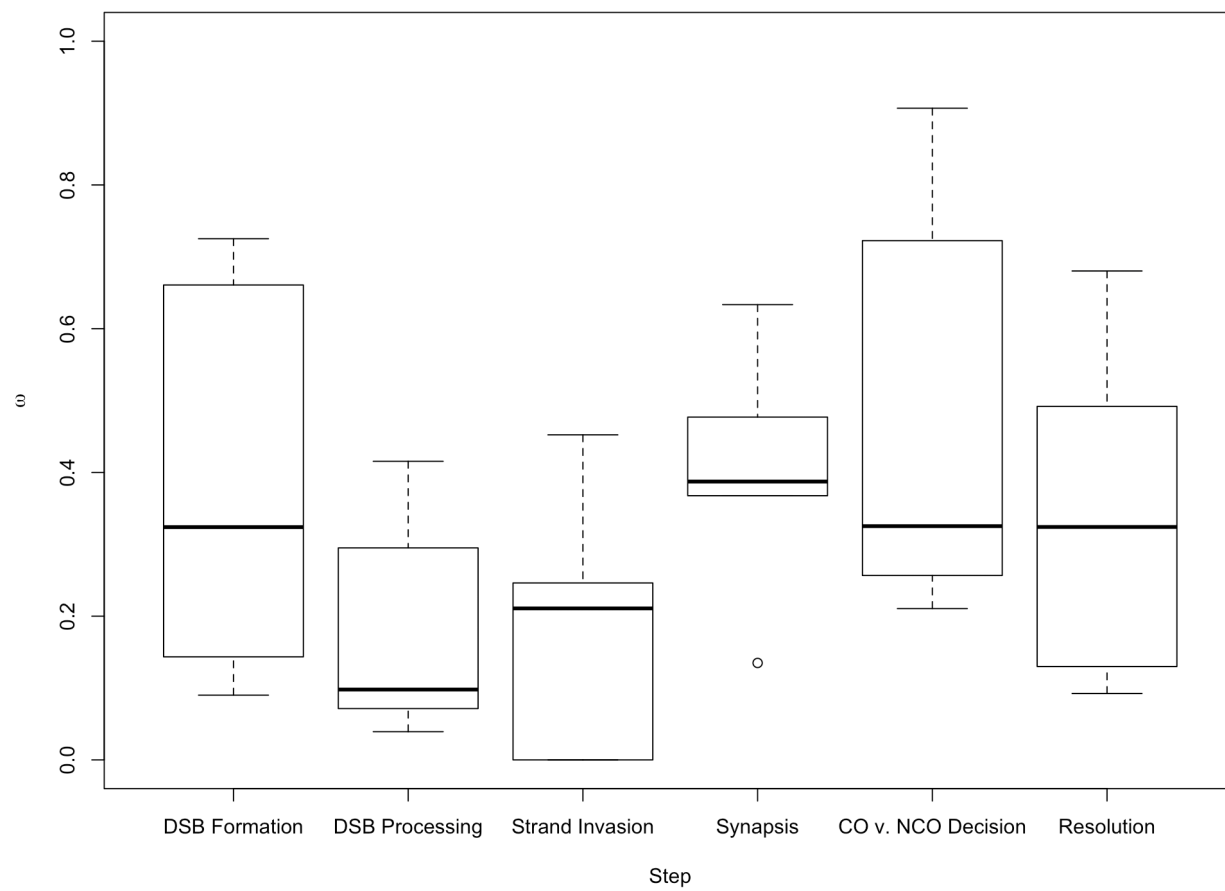
313

314 **Figure 5:** High concordance between there rate of evolution of recombination gene between human and
 315 macaques and the rate of evolution among mammals. The linear regression is shown in red and the 1:1 line is
 316 shown as a dashed line.



317

318 **Figure 6:** Distribution of ω by step in recombination pathway.



319

Table 3: PAML analysis of 32 recombination genes in mammals (Yang 2007).

<i>Gene</i>	<i>bp</i>	<i>N</i>	ω	<i>M</i>	<i>M1-M2</i>	<i>p-value</i>	<i>M7-M8</i>	<i>p-value</i>	<i>M8a-M8</i>	<i>p-value</i>
A)										
<i>HORMAD1</i>	1212	16	0.3036	7	0	1.000	1.795	0.4076	—	—
<i>MEI4</i>	1170	16	0.4332	7	0	1.000	0.005	0.9976	—	—
<i>REC114</i>	870	15	0.4003	7	0	1.000	5.384	0.0677	—	—
<i>IHO1</i>	1824	16	0.7095	8	13.061	0.0015	17.571	0.0002	14.527	0.0001
<i>SPO11</i>	1188	15	0.1654	7	0	1.000	4.648	0.0980	—	—
B)										
<i>HORMAD2</i>	981	15	0.3153	7	0	1.000	3.650	0.1612	—	—
<i>MRE11</i>	2136	16	0.1688	8	0.363	0.8342	11.931	0.0026	4.706	0.0301
<i>NBS1</i>	2289	15	0.4183	8	0	1.000	12.763	0.0017	4.087	0.0432
<i>RAD50</i>	3936	16	0.1006	7	0	1.000	0.301	0.8605	—	—
<i>BRCC3</i>	954	15	0.0602	7	0	1.000	0.250	0.8826	—	—
C)										
<i>DMC1</i>	1020	15	0.0351	1	0.488	0.7835	5.000	0.0821	—	—
<i>RAD51</i>	1017	16	0.0268	7	0	1.000	0	1.000	—	—
<i>SPATA22</i>	1101	16	0.4893	7	0	1.000	0.429	0.8070	—	—
<i>MEIOB</i>	1425	16	0.2341	7	0	1.000	0.665	0.7172	—	—
<i>MCMD2</i>	2052	16	0.2239	7	0	1.000	0.628	0.7307	—	—
D)										
<i>REC8</i>	1833	16	0.3698	8	0	1.000	14.690	0.0006	5.927	0.0149
<i>RAD21L</i>	1686	15	0.503	8	12.124	0.0023	32.050	>0.0001	12.049	0.0005
<i>SYCP1</i>	3015	16	0.4337	8	8.711	0.0128	26.860	>0.0001	9.243	0.0024
<i>SYCP2</i>	4650	16	0.5572	8	11.584	0.0031	37.200	>0.0001	15.838	0.0001
<i>TEX12</i>	369	14	0.2297	7	0.0565	0.9721	1.549	0.4610	—	—
E)										
<i>TEX11</i>	2844	15	0.8483	8	60.872	>0.0001	82.665	>0.0001	61.141	>0.0001
<i>SHOC1</i>	4644	16	0.6113	8	12.447	0.0020	30.561	>0.0001	15.645	0.0001
<i>RNF212</i>	948	16	0.5014	8	0	1.000	16.366	0.0003	5.202	0.0226
<i>RNF212B</i>	906	14	0.4066	7	0	1.000	0.500	0.7788	—	—
<i>MSH4</i>	2814	16	0.2132	8	16.608	0.0002	39.447	>0.0001	23.238	>0.0001

<i>Gene</i>	<i>bp</i>	<i>N</i>	ω	<i>M</i>	<i>M1-M2</i>	<i>p-value</i>	<i>M7-M8</i>	<i>p-value</i>	<i>M8a-M8</i>	<i>p-value</i>
<i>MSH5</i>	2565	15	0.1642	7	0	<i>1.000</i>	4.214	<i>0.1216</i>	—	—
F)										
<i>MER3</i>	4458	16	0.3633	8a	0	<i>1.000</i>	12.838	<i>0.0016</i>	3.109	<i>0.0779</i>
<i>CNTD1</i>	1026	15	0.2496	7	0	<i>1.000</i>	0.936	<i>0.6263</i>	—	—
<i>HEI10</i>	831	15	0.1226	7	0	<i>1.000</i>	0.250	<i>0.8826</i>	—	—
<i>MLH1</i>	2313	15	0.1652	8a	0	<i>1.000</i>	12.221	<i>0.0022</i>	0.280	<i>0.5970</i>
<i>MLH3</i>	4419	16	0.4444	7	0	<i>1.000</i>	3.757	<i>0.1528</i>	—	—
<i>MUS81</i>	1665	16	0.2124	7	0	<i>1.000</i>	0.628	<i>0.7304</i>	—	—

321 **Table 4:** Polymorphism & Divergence Data

<i>Gene</i>	ω	<i>Pn</i>	<i>Ps</i>	<i>Pn/Ps</i>	<i>Dn</i>	<i>Ds</i>	<i>Dn/Ds</i>	<i>MK Test</i>	α	<i>NI</i>	
A)											
<i>HORMAD1</i>	0.0901	84	35	2.4000	5	12	0.4167	0.0018	-4.7600	5.7600	Neg.
<i>MEI4</i>	0.7252	15	7	2.1429	24	9	2.6667	0.7679	0.1964	0.8036	—
<i>REC114</i>	0.3239	76	37	2.0541	11	14	0.7857	0.0392	-1.6143	2.6143	Neg.
<i>IHO1</i>	0.6608	130	64	2.0313	36	19	1.8947	0.8718	-0.0720	1.0720	—
<i>SPO11</i>	0.1434	118	52	2.2692	11	22	0.5000	0.0001	-3.5385	4.5385	Neg.
B)											
<i>HORMAD2</i>	0.2950	80	31	2.5806	7	9	0.7778	0.0404	-2.3180	3.3180	Neg.
<i>MRE11</i>	0.0392	211	86	2.4535	5	35	0.1429	>0.0001	-16.1744	17.1744	Neg.
<i>NBS1</i>	0.4155	221	93	2.3763	34	25	1.3600	0.0666	-0.7473	1.7473	—
<i>RAD50</i>	0.0714	303	118	2.5678	8	43	0.1860	>0.0001	-12.8019	13.8019	Neg.
<i>BRCC3</i>	0.0979	13	21	0.6190	2	6	0.3333	0.6888	-0.8571	1.8571	—
C)											
<i>DMC1</i>	0.0000	72	42	1.7143	0	11	0.0000	>0.0001	—	—	Neg.
<i>RAD51</i>	0.0000	50	48	1.0417	0	13	0.0000	>0.0001	—	—	Neg.
<i>SPATA22</i>	0.4523	114	45	2.5333	21	10	2.1000	0.6700	-0.2063	1.2063	—
<i>MEIOB</i>	0.2462	91	40	2.2750	20	22	0.9091	0.0200	-1.5025	2.5025	Neg.
<i>MCMDC2</i>	0.2108	165	54	3.0556	16	26	0.6154	>0.0001	-3.9653	4.9653	Neg.
D)											
<i>REC8</i>	0.4770	147	76	1.9342	38	31	1.2258	0.1164	-0.5779	1.5779	—
<i>RAD21L</i>	0.6334	51	17	3.000	27	13	2.0769	0.5051	-0.4444	1.4444	—
<i>SYCP1</i>	0.3676	213	100	2.1300	33	37	1.2222	0.0546	-0.7427	1.7427	—
<i>SYCP2</i>	0.3873	429	154	2.8506	74	53	1.3962	0.0005	-1.0417	2.0417	Neg.
<i>TEX12</i>	0.1349	31	16	1.9375	2	4	0.5000	0.1836	-2.875	3.875	—
E)											
<i>TEX11</i>	0.9068	126	81	1.5556	55	25	2.200	0.2234	0.2929	0.7071	—
<i>SHOC1</i>	0.7225	368	124	2.9677	85	37	2.2973	0.2521	-0.2918	1.2918	—
<i>RNF212</i>	0.3870	—	—	—	17	18	0.9444	—	—	—	—
<i>RNF212B</i>	0.2566	368	124	2.9677	8	12	0.6667	0.0013	-3.4516	4.4516	Neg.
<i>MSH4</i>	0.2635	260	94	2.7660	24	29	0.8276	>0.0001	-2.3422	3.3422	Neg.

<i>Gene</i>	ω	<i>Pn</i>	<i>Ps</i>	<i>Pn/Ps</i>	<i>Dn</i>	<i>Ds</i>	<i>Dn/Ds</i>	<i>MK Test</i>	α	<i>NI</i>	
<i>MSH5</i>	0.2106	197	104	1.8942	19	33	0.5758	0.0002	-2.2900	3.2900	Neg.
F)											
<i>MER3</i>	0.3247	402	143	2.8112	54	44	1.2273	0.0004	-1.2906	2.2906	Neg.
<i>CNTD1</i>	0.6803	81	47	1.7234	13	8	1.6250	<i>1.0000</i>	-0.0606	1.0606	—
<i>HEI10</i>	0.3235	73	33	2.2121	4	5	0.8000	<i>0.1541</i>	-1.7652	2.7652	—
<i>MLH1</i>	0.0924	255	90	2.8333	9	29	0.3103	>0.0001	-8.1296	9.1296	Neg.
<i>MLH3</i>	0.4919	437	167	2.6168	77	57	1.3509	0.0012	-0.9370869	1.937087	Neg.
<i>MUS81</i>	0.1299	208	81	2.5679	17	40	0.4250	>0.0001	-5.0421	6.0421	Neg.

Table 5: PAML - MNM Analysis

<i>Gene</i>	<i>bp</i>	<i>N</i>	ω	<i>M</i>	<i>M1-M2</i>	<i>p-value</i>	<i>M7-M8</i>	<i>p-value</i>	<i>M8a-M8</i>	<i>p-value</i>
<i>IHO1</i>	1824	16	0.6104	7	0	<i>1.000</i>	0.258	<i>0.8789</i>	—	—
<i>MRE11</i>	2136	16	0.1330	7	0.226	<i>0.8930</i>	3.056	<i>0.2169</i>	—	—
<i>NBS1</i>	2289	15	0.3413	7	0	<i>1.000</i>	1.956	<i>0.3761</i>	—	—
<i>REC8</i>	1833	16	0.2905	7	0	<i>1.000</i>	5.321	<i>0.0699</i>	—	—
<i>RAD21L</i>	1686	15	0.4271	8a	2.329	<i>0.3121</i>	9.497	<i>0.0087</i>	1.620	<i>0.2031</i>
<i>SYCP1</i>	3015	16	0.3731	8a	3.328	<i>0.1893</i>	13.440	<i>0.0012</i>	2.122	<i>0.1452</i>
<i>SYCP2</i>	4650	16	0.4752	7	0	<i>1.000</i>	1.758	<i>0.4151</i>	—	—
<i>TEX11</i>	2844	15	0.7287	8	9.989	<i>0.0068</i>	18.776	<i>0.0001</i>	10.656	<i>0.0011</i>
<i>SHOC1</i>	4644	16	0.5519	8a	0	<i>1.000</i>	7.439	<i>0.0242</i>	0.292	<i>0.5887</i>
<i>RNF212</i>	948	16	0.3685	7	0	<i>1.000</i>	0	<i>1.000</i>	—	—
<i>MSH4</i>	2814	16	0.1509	7	0	<i>1.000</i>	2.079	<i>0.3536</i>	—	—

Acknowledgements

A.L.D. was supported by NHGRI Training Grant to the Genomic Sciences Training Program 5T32HG002760.
B.A.P. was supported by NIH grant R01 GM100426A and NSF grant DEB 1353737.

References

- Abascal F., R. Zardoya, and M. J. Telford, 2010 TranslatorX: Multiple alignment of nucleotide sequences guided by amino acid translations. *Nucleic acids research* 38: W7–W13.
- Baker S. M., A. W. Plug, T. A. Prolla, C. E. Bronner, and A. C. Harris *et al.*, 1996 Involvement of mouse *mlh1* in dna mismatch repair and meiotic crossing over. *Nature genetics* 13: 336.
- Balcova M., B. Faltusova, V. Gergelits, T. Bhattacharyya, and O. Mihola *et al.*, 2016 Hybrid sterility locus on chromosome x controls meiotic recombination rate in mouse. *PLoS genetics* 12: e1005906.
- Barbosa-Morais N. L., M. Irimia, Q. Pan, H. Y. Xiong, and S. Gueroussov *et al.*, 2012 The evolutionary landscape of alternative splicing in vertebrate species. *Science* 338: 1587–1593.
- Barrett T., S. E. Wilhite, P. Ledoux, C. Evangelista, and I. F. Kim *et al.*, 2012 NCBI geo: Archive for functional genomics data sets—update. *Nucleic acids research* 41: D991–D995.
- Baudat F., K. Manova, J. P. Yuen, M. Jasin, and S. Keeney, 2000 Chromosome synapsis defects and sexually dimorphic meiotic progression in mice lacking *spo11*. *Molecular cell* 6: 989–998.
- Baudat F., and B. de Massy, 2007 Regulating double-stranded dna break repair towards crossover or non-crossover during mammalian meiosis. *Chromosome research* 15: 565–577.
- Begun D. J., and C. F. Aquadro, 1992 Levels of naturally occurring dna polymorphism correlate with recombination rates in *D. Melanogaster*. *Nature* 356: 519.
- Bergerat A., B. de Massy, D. Gadelle, P.-C. Varoutas, and A. Nicolas *et al.*, 1997 An atypical topoisomerase ii from archaea with implications for meiotic recombination. *Nature* 386: 414.
- Besenbacher S., P. Sulem, A. Helgason, H. Helgason, and H. Kristjansson *et al.*, 2016 Multi-nucleotide de novo mutations in humans. *PLoS genetics* 12: e1006315.
- Bisig C. G., M. F. Guiraldelli, A. Kouznetsova, H. Scherthan, and C. Höög *et al.*, 2012 Synaptonemal complex components persist at centromeres and are required for homologous centromere pairing in mouse spermatocytes. *PLoS genetics* 8: e1002701.

350 Bolcun-Filas E., and J. C. Schimenti, 2012 Genetics of meiosis and recombination in mice. *International*
351 *review of cell and molecular biology* 298: 179–227.

352 Brand C. L., M. V. Cattani, S. B. Kingan, E. L. Landeen, and D. C. Presgraves, 2018 Molecular evolution at
353 a meiosis gene mediates species differences in the rate and patterning of recombination. *Current Biology* 28:
354 1289–1295.

355 Broman K. W., J. C. Murray, V. C. Sheffield, R. L. White, and J. L. Weber, 1998 Comprehensive human
356 genetic maps: Individual and sex-specific variation in recombination. *The American Journal of Human*
357 *Genetics* 63: 861–869.

358 Brown M. S., and D. K. Bishop, 2014 DNA strand exchange and recombination in meiosis. *Cold Spring*
359 *Harbor perspectives in biology* a016659.

360 Burt A., and G. Bell, 1987 Red queen versus tangled bank models. *Nature* 330: 118.

361 Charlesworth B., M. Morgan, and D. Charlesworth, 1993 The effect of deleterious mutations on neutral
362 molecular variation. *Genetics* 134: 1289–1303.

363 Charlesworth B., P. Jarne, and S. Assimakopoulos, 1994 The distribution of transposable elements within and
364 between chromosomes in a population of *Drosophila melanogaster*. III. Element abundances in heterochromatin.
365 *Genetics Research* 64: 183–197.

366 Chen M.-Y., D. Liang, and P. Zhang, 2017 Phylogenomic resolution of the phylogeny of Laurasiatherian
367 mammals: Exploring phylogenetic signals within coding and noncoding sequences. *Genome biology and*
368 *evolution* 9: 1998–2012.

369 Chowdhury R., P. R. Bois, E. Feingold, S. L. Sherman, and V. G. Cheung, 2009 Genetic analysis of variation
370 in human meiotic recombination. *PLoS genetics* 5: e1000648.

371 Clark N. L., E. Alani, and C. F. Aquadro, 2012 Evolutionary rate covariation reveals shared functionality
372 and coexpression of genes. *Genome research*.

373 Clark N. L., E. Alani, and C. F. Aquadro, 2013 Evolutionary rate covariation in meiotic proteins results from
374 fluctuating evolutionary pressure in yeasts and mammals. *Genetics* 193: 529–538.

375 Cloud V., Y.-L. Chan, J. Grubb, B. Budke, and D. K. Bishop, 2012 Rad51 is an accessory factor for
376 dmc1-mediated joint molecule formation during meiosis. *Science* 337: 1222–1225.

377 Comeron J. M., M. Kreitman, and M. Aguadé, 1999 Natural selection on synonymous sites is correlated with
378 gene length and recombination in *Drosophila*. *Genetics* 151: 239–249.

379 Comeron J. M., R. Ratnappan, and S. Bailin, 2012 The many landscapes of recombination in drosophila
380 melanogaster. PLoS genetics 8: e1002905.

381 Coop G., and M. Przeworski, 2007 An evolutionary view of human recombination. Nature Reviews Genetics
382 8: 23.

383 Costa Y., R. Speed, R. Öllinger, M. Alsheimer, and C. A. Semple *et al.*, 2005 Two novel proteins recruited by
384 synaptonemal complex protein 1 (sycp1) are at the centre of meiosis. Journal of cell science 118: 2755–2762.

385 Dapper A. L., and B. A. Payseur, 2017 Connecting theory and data to understand recombination rate
386 evolution. Phil. Trans. R. Soc. B 372: 20160469.

387 Dumont B. L., and B. A. Payseur, 2010 Evolution of the genomic recombination rate in murid rodents.
388 Genetics.

389 Dumont B. L., M. A. White, B. Steffy, T. Wiltshire, and B. A. Payseur, 2011 Extensive recombination
390 rate variation in the house mouse species complex inferred from genetic linkage maps. Genome research 21:
391 114–125.

392 Duret L., and P. F. Arndt, 2008 The impact of recombination on nucleotide substitutions in the human
393 genome. PLoS genetics 4: e1000071.

394 Edelman W., P. E. Cohen, M. Kane, K. Lau, and B. Morrow *et al.*, 1996 Meiotic pachytene arrest in
395 mlh1-deficient mice. Cell 85: 1125–1134.

396 Edgar R. C., 2004 MUSCLE: Multiple sequence alignment with high accuracy and high throughput. Nucleic
397 acids research 32: 1792–1797.

398 Fan Y., Z.-Y. Huang, C.-C. Cao, C.-S. Chen, and Y.-X. Chen *et al.*, 2013 Genome of the chinese tree shrew.
399 Nature communications 4: 1426.

400 Felsenstein J., 1974 The evolutionary advantage of recombination. Genetics 78: 737–756.

401 Finsterbusch F., R. Ravindranathan, I. Dereli, M. Stanzione, and D. Tränkner *et al.*, 2016 Alignment
402 of homologous chromosomes and effective repair of programmed dna double-strand breaks during mouse
403 meiosis require the minichromosome maintenance domain containing 2 (mcm2) protein. PLoS genetics 12:
404 e1006393.

405 Fledel-Alon A., E. M. Leffler, Y. Guan, M. Stephens, and G. Coop *et al.*, 2011 Variation in human
406 recombination rates and its genetic determinants. PLoS one 6: e20321.

407 Fraune J., M. Alsheimer, J. Redolfi, C. Brochier-Armanet, and R. Benavente, 2014 Protein sycp2 is an ancient
 408 component of the metazoan synaptonemal complex. *Cytogenetic and genome research* 144: 299–305.

409 Gonen S., M. Battagin, S. E. Johnston, G. Gorjanc, and J. M. Hickey, 2017 The potential of shifting
 410 recombination hotspots to increase genetic gain in livestock breeding. *Genetics Selection Evolution* 49: 55.

411 Grey C., P. Barthès, Chauveau-Le Friec G., F. Langa, and F. Baudat *et al.*, 2011 Mouse prdm9 dna-binding
 412 specificity determines sites of histone h3 lysine 4 trimethylation for initiation of meiotic recombination. *PLoS*
 413 *biology* 9: e1001176.

414 Grey C., F. Baudat, and B. de Massy, 2018 PRDM9, a driver of the genetic map. *PLoS genetics* 14: e1007479.

415 Hamer G., K. Gell, A. Kouznetsova, I. Novak, and R. Benavente *et al.*, 2006 Characterization of a novel
 416 meiosis-specific protein within the central element of the synaptonemal complex. *Journal of cell science* 119:
 417 4025–4032.

418 Hassold T., and P. Hunt, 2001 To err (meiotically) is human: The genesis of human aneuploidy. *Nature*
 419 *Reviews Genetics* 2: 280.

420 Hernández-Hernández A., S. Masich, T. Fukuda, A. Kouznetsova, and S. Sandin *et al.*, 2016 The central
 421 element of the synaptonemal complex in mice is organized as a bilayered junction structure. *J Cell Sci* 129:
 422 2239–2249.

423 Hill W. G., and A. Robertson, 1966 The effect of linkage on limits to artificial selection. *Genetics Research* 8:
 424 269–294.

425 Hunter C. M., W. Huang, T. F. Mackay, and N. D. Singh, 2016 The genetic architecture of natural variation
 426 in recombination rate in *drosophila melanogaster*. *PLoS genetics* 12: e1005951.

427 Jeffreys A. J., R. Neumann, M. Panayi, S. Myers, and P. Donnelly, 2005 Human recombination hot spots
 428 hidden in regions of strong marker association. *Nature genetics* 37: 601.

429 Johnston S. E., C. Bérénos, J. Slate, and J. M. Pemberton, 2016 Conserved genetic architecture underlying
 430 individual recombination rate variation in a wild population of soay sheep (*ovis aries*). *Genetics* 198: 111–115.

431 Johnston S. E., J. Huisman, and J. M. Pemberton, 2018 A genomic region containing *rec8* and *rnf212b* is
 432 associated with individual recombination rate variation in a wild population of red deer (*cervus elaphus*). *G3:*
 433 *Genes, Genomes, Genetics* 8: 2000063.

434 Kadri N. K., C. Harland, P. Faux, N. Cambisano, and L. Karim *et al.*, 2016 Coding and noncoding variants
 435 in *hfm1*, *mlh3*, *msh4*, *msh5*, *rnf212*, and *rnf212b* affect recombination rate in cattle. *Genome research*.

Keeney S., C. N. Giroux, and N. Kleckner, 1997 Meiosis-specific dna double-strand breaks are catalyzed by spo11, a member of a widely conserved protein family. *Cell* 88: 375–384.

Keeney S., 2007 Spo11 and the formation of dna double-strand breaks in meiosis, pp. 81–123 in *Recombination and meiosis*, Springer.

Kobayashi W., M. Takaku, S. Machida, H. Tachiwana, and K. Maehara *et al.*, 2016 Chromatin architecture may dictate the target site for dmc1, but not for rad51, during homologous pairing. *Scientific reports* 6: 24228.

Kong A., G. Thorleifsson, H. Stefansson, G. Masson, and A. Helgason *et al.*, 2008 Sequence variants in the rnf212 gene associate with genome-wide recombination rate. *Science* 319: 1398–1401.

Kong A., G. Thorleifsson, D. F. Gudbjartsson, G. Masson, and A. Sigurdsson *et al.*, 2010 Fine-scale recombination rate differences between sexes, populations and individuals. *Nature* 467: 1099.

Kong A., G. Thorleifsson, M. L. Frigge, G. Masson, and D. F. Gudbjartsson *et al.*, 2014 Common and low-frequency variants associated with genome-wide recombination rate. *Nature genetics* 46: 11.

Kumar R., N. Ghyselinck, K.-i. Ishiguro, Y. Watanabe, and A. Kouznetsova *et al.*, 2015 MEI4: A central player in the regulation of meiotic dna double strand break formation in the mouse. *J Cell Sci* jcs-165464.

Lange J., S. Yamada, S. E. Tischfield, J. Pan, and S. Kim *et al.*, 2016 The landscape of mouse meiotic double-strand break formation, processing, and repair. *Cell* 167: 695–708.

Langmead B., and S. L. Salzberg, 2012 Fast gapped-read alignment with bowtie 2. *Nature methods* 9: 357.

La Salle S., K. Palmer, O’Brien M., J. C. Schimenti, and J. Eppig *et al.*, 2012 Spata22, a novel vertebrate-specific gene, is required for meiotic progress in mouse germ cells. *Biology of reproduction* 86: 45–1.

Latrille T., L. Duret, and N. Lartillot, 2017 The red queen model of recombination hot-spot evolution: A theoretical investigation. *Phil. Trans. R. Soc. B* 372: 20160463.

Leinonen R., H. Sugawara, M. Shumway, and I. N. S. D. Collaboration, 2010 The sequence read archive. *Nucleic acids research* 39: D19–D21.

Lesecque Y., S. Glémin, N. Lartillot, D. Mouchiroud, and L. Duret, 2014 The red queen model of recombination hotspots evolution in the light of archaic and modern human genomes. *PLoS genetics* 10: e1004790.

Li H., B. Handsaker, A. Wysoker, T. Fennell, and J. Ruan *et al.*, 2009 The sequence alignment/map format and samtools. *Bioinformatics* 25: 2078–2079.

464 Lipkin S. M., P. B. Moens, V. Wang, M. Lenzi, and D. Shanmugarajah *et al.*, 2002 Meiotic arrest and
465 aneuploidy in *mlh3*-deficient mice. *Nature genetics* 31: 385.

466 Ma L., O’Connell J. R., P. M. VanRaden, B. Shen, and A. Padhi *et al.*, 2015 Cattle sex-specific recombination
467 and genetic control from a large pedigree analysis. *PLoS genetics* 11: e1005387.

468 Meuwissen R., H. H. Offenberg, A. Dietrich, A. Riesewijk, and M. van Iersel *et al.*, 1992 A coiled-coil related
469 protein specific for synapsed regions of meiotic prophase chromosomes. *The EMBO Journal* 11: 5091.

470 Murdoch B., N. Owen, S. Shirley, S. Crumb, and K. W. Broman *et al.*, 2010 Multiple loci contribute to
471 genome-wide recombination levels in male mice. *Mammalian genome* 21: 550–555.

472 Myers S., R. Bowden, A. Tumian, R. E. Bontrop, and C. Freeman *et al.*, 2010 Drive against hotspot motifs
473 in primates implicates the *prdm9* gene in meiotic recombination. *Science* 327: 876–879.

474 Oh J., A. Al-Zain, E. Cannavo, P. Cejka, and L. S. Symington, 2016 *Xrs2* dependent and independent
475 functions of the *mre11-rad50* complex. *Molecular cell* 64: 405–415.

476 Oliver P. L., L. Goodstadt, J. J. Bayes, Z. Birtle, and K. C. Roach *et al.*, 2009 Accelerated evolution of the
477 *prdm9* speciation gene across diverse metazoan taxa. *PLoS genetics* 5: e1000753.

478 Pamilo P., and M. Nei, 1988 Relationships between gene trees and species trees. *Molecular biology and*
479 *evolution* 5: 568–583.

480 Pan Q., O. Shai, L. J. Lee, B. J. Frey, and B. J. Blencowe, 2008 Deep surveying of alternative splicing
481 complexity in the human transcriptome by high-throughput sequencing. *Nature genetics* 40: 1413.

482 Parvanov E. D., P. M. Petkov, and K. Paigen, 2010 *Prdm9* controls activation of mammalian recombination
483 hotspots. *Science* 327: 835–835.

484 Perelman P., W. E. Johnson, C. Roos, H. N. Seuánez, and J. E. Horvath *et al.*, 2011 A molecular phylogeny
485 of living primates. *PLoS genetics* 7: e1001342.

486 Petit M., J.-M. Astruc, J. Sarry, L. Drouilhet, and S. Fabre *et al.*, 2017 Variation in recombination rate and
487 its genetic determinism in sheep populations. *Genetics* genetics–300123.

488 Prasad A. B., M. W. Allard, N. C. S. Program, and E. D. Green, 2008 Confirming the phylogeny of mammals
489 by use of large comparative sequence data sets. *Molecular Biology and Evolution* 25: 1795–1808.

490 Priedigkeit N., N. Wolfe, and N. L. Clark, 2015 Evolutionary signatures amongst disease genes permit novel
491 methods for gene prioritization and construction of informative gene-based networks. *PLoS genetics* 11:
492 e1004967.

493 Rao H. P., H. Qiao, S. K. Bhatt, L. R. Bailey, and H. D. Tran *et al.*, 2017 A sumo-ubiquitin relay recruits
494 proteasomes to chromosome axes to regulate meiotic recombination. *Science* 355: 403–407.

495 Reynolds A., H. Qiao, Y. Yang, J. K. Chen, and N. Jackson *et al.*, 2013 RNF212 is a dosage-sensitive regulator
496 of crossing-over during mammalian meiosis. *Nature genetics* 45: 269.

497 Rogacheva M. V., C. M. Manhart, C. Chen, A. Guarne, and J. Surtees *et al.*, 2014 Mlh1-mlh3, a meiotic
498 crossover and dna mismatch repair factor, is a msh2-msh3-stimulated endonuclease. *Journal of Biological*
499 *Chemistry* jbc-M113.

500 Romanienko P. J., and R. D. Camerini-Otero, 2000 The mouse spo11 gene is required for meiotic chromosome
501 synapsis. *Molecular cell* 6: 975–987.

502 Ronquist F., M. Teslenko, Van Der Mark P., D. L. Ayres, and A. Darling *et al.*, 2012 MrBayes 3.2: Efficient
503 bayesian phylogenetic inference and model choice across a large model space. *Systematic biology* 61: 539–542.

504 Rosenberg N. A., 2002 The probability of topological concordance of gene trees and species trees. *Theoretical*
505 *population biology* 61: 225–247.

506 Sandor C., W. Li, W. Coppieters, T. Druet, and C. Charlier *et al.*, 2012 Genetic variants in rec8, rnf212, and
507 prdm9 influence male recombination in cattle. *PLoS genetics* 8: e1002854.

508 Schmekel K., and B. Daneholt, 1995 The central region of the synaptonemal complex revealed in three
509 dimensions. *Trends in cell biology* 5: 239–242.

510 Schramm S., J. Fraune, R. Naumann, A. Hernandez-Hernandez, and C. Höög *et al.*, 2011 A novel mouse
511 synaptonemal complex protein is essential for loading of central element proteins, recombination, and fertility.
512 *PLoS genetics* 7: e1002088.

513 Schrider D. R., J. N. Hourmozdi, and M. W. Hahn, 2011 Pervasive multinucleotide mutational events in
514 eukaryotes. *Current Biology* 21: 1051–1054.

515 Scornavacca C., and N. Galtier, 2017 Incomplete lineage sorting in mammalian phylogenomics. *Systematic*
516 *biology* 66: 112–120.

517 Segura J., L. Ferretti, S. Ramos-Onsins, L. Capilla, and M. Farré *et al.*, 2013 Evolution of recombination in
518 eutherian mammals: Insights into mechanisms that affect recombination rates and crossover interference.
519 *Proceedings of the Royal Society of London B: Biological Sciences* 280: 20131945.

520 Shen B., J. Jiang, E. Seroussi, G. E. Liu, and L. Ma, 2018 Characterization of recombination features and
521 the genetic basis in multiple cattle breeds. *BMC genomics* 19: 304.

Smukowski C., and M. Noor, 2011 Recombination rate variation in closely related species. *Heredity* 107: 496.

Snowden T., S. Acharya, C. Butz, M. Berardini, and R. Fishel, 2004 HSMH4-hSMH5 recognizes holliday junctions and forms a meiosis-specific sliding clamp that embraces homologous chromosomes. *Molecular cell* 15: 437–451.

Stanzione M., M. Baumann, F. Papanikos, I. Dereli, and J. Lange *et al.*, 2016 Meiotic dna break formation requires the unsynapsed chromosome axis-binding protein iho1 (ccdc36) in mice. *Nature cell biology* 18: 1208.

Stapley J., P. G. Feulner, S. E. Johnston, A. W. Santure, and C. M. Smadja, 2017 Variation in recombination frequency and distribution across eukaryotes: Patterns and processes. *Phil. Trans. R. Soc. B* 372: 20160455.

Thorvaldsdóttir H., J. T. Robinson, and J. P. Mesirov, 2013 Integrative genomics viewer (igv): High-performance genomics data visualization and exploration. *Briefings in bioinformatics* 14: 178–192.

Trapnell C., L. Pachter, and S. L. Salzberg, 2009 TopHat: Discovering splice junctions with rna-seq. *Bioinformatics* 25: 1105–1111.

Ubeda F., and J. Wilkins, 2011 The red queen theory of recombination hotspots. *Journal of evolutionary biology* 24: 541–553.

Venkat A., M. W. Hahn, and J. W. Thornton, 2018 Multinucleotide mutations cause false inferences of lineage-specific positive selection. *Nature ecology & evolution* 2: 1280.

Vries S. S. de, E. B. Baart, M. Dekker, A. Siezen, and D. G. de Rooij *et al.*, 1999 Mouse muts-like protein msh5 is required for proper chromosome synapsis in male and female meiosis. *Genes & Development* 13: 523–531.

Vries F. A. de, E. de Boer, M. van den Bosch, W. M. Baarends, and M. Ooms *et al.*, 2005 Mouse sycp1 functions in synaptonemal complex assembly, meiotic recombination, and xy body formation. *Genes & development* 19: 1376–1389.

Ward J. O., L. G. Reinholdt, W. W. Motley, L. M. Niswander, and D. C. Deacon *et al.*, 2007 Mutation in mouse hei10, an e3 ubiquitin ligase, disrupts meiotic crossing over. *PLoS genetics* 3: e139.

Wheeler D. L., T. Barrett, D. A. Benson, S. H. Bryant, and K. Canese *et al.*, 2006 Database resources of the national center for biotechnology information. *Nucleic acids research* 35: D5–D12.

Xu Y., R. A. Greenberg, E. Schonbrunn, and P. J. Wang, 2017 Meiosis-specific proteins meiob and spata22 cooperatively associate with the single-stranded dna-binding replication protein a complex and dna double-strand breaks. *Biology of reproduction* 96: 1096–1104.

551 Yang Z., 1997 PAML: A program package for phylogenetic analysis by maximum likelihood. *Bioinformatics*
552 13: 555–556.

553 Yang F., De La Fuente R., N. A. Leu, C. Baumann, and K. J. McLaughlin *et al.*, 2006 Mouse sycp2 is required
554 for synaptonemal complex assembly and chromosomal synapsis during male meiosis. *The Journal of Cell*
555 *Biology* 173: 497–507.

556 Yang Z., 2007 PAML 4: Phylogenetic analysis by maximum likelihood. *Molecular Biology and Evolution* 24:
557 1586–1591. <https://doi.org/10.1093/molbev/msm088>

558 Yang F., K. Gell, Van Der Heijden G. W., S. Eckardt, and N. A. Leu *et al.*, 2008 Meiotic failure in male mice
559 lacking an x-linked factor. *Genes & development* 22: 682–691.

560 Zerbino D. R., P. Achuthan, W. Akanni, M. R. Amode, and D. Barrell *et al.*, 2017 Ensembl 2018. *Nucleic*
561 *acids research* 46: D754–D761.